Beam propagation in two-dimensional media with spatial dispersion

Zhiping Dai,[1,2] Yi Xu,[1] Qi Guo,[1,*] and Sien Chi[3]

[1]*Laboratory of Nanophotonic Functional Materials and Devices, South China Normal University, Guangzhou, Guangdong, China*

[2]*Department of Physics and Electronic Information Science, Hengyang Normal University, Hengyang, Hunan, China*

[3]*Institute of Electro-Optical Engineering, National Chiao Tung University, Hsinchu, Taiwan*

(Received 20 January 2013; published 22 May 2013)

We theoretically investigate the propagation of a paraxial beam in two-dimensional media with spatial dispersion. Based on the spatial dispersion theory and the $(1 + 1)$-dimensional paraxial wave equation, we get an expression which determines the diffraction of the beam. By fitting the dispersion surface of a typical spatial dispersion medium (a photonic crystal) calculated by the plane-wave-expansion method, the value of the diffraction term is determined, with which one can predict the diffraction of the paraxial beam that propagates in such media. Numerical simulations based on the finite-difference time-domain method confirm the theoretical results.

DOI: 10.1103/PhysRevA.87.053827 PACS number(s): 42.25.Bs, 71.36.+c, 78.20.Ci, 71.35.−y

I. INTRODUCTION

Spatial dispersion (SD), first quantitatively described by Ginzburg more than 50 years ago [1], arises from the dependence of the permittivity on the wave vector **k** at a fixed frequency of light. Media exhibiting this behavior are also termed "(linearly) nonlocal" due to the fact that the linear polarization at a given spatial location **r** depends on the electric field over a finite volume surrounding that point. Linear nonlocality and SD are two terms for the same physical phenomenon, referring to direct **r** space and reciprocal **k** space, respectively [2,3].

With the explosive development of artificial materials in recent years, SD becomes a common phenomenon since one can construct a material with periods and features comparable to the interest wavelength [4]. In particular, it has been shown that a thin-wire metamaterial exhibits strong SD even in the quasistatic limit for the incident wave that the electric field is not exactly parallel to the wires [5,6]. A cubic crystal with SD could mimic such a wire-mesh metamaterial [7]. In principle, the structures of the artificial materials have an effect on the properties of SD. Even small features in the unit cell could produce a SD effect [8,9].

At the same time, diffraction management is an active area of research since it enables the realization of all-optical circuits and the efficient implementation of high-resolution imaging, which requires precise control of the beam size. It is well known that an electromagnetic beam suffers from diffraction when it propagates in homogeneous and linear dielectric materials. No material can preserve the size of a beam unless a specific structure or nonlinearity is employed. As we know, diffraction would reduce the power efficiency when we use light as the carrier to realize information exchange between two optical circuits [10]. Specifically, in linear media, the simplest way of diffraction suppression is to use a waveguide, whose refractive index spatial profile is used to trap a beam and thereby halt its spreading. Controllable diffraction of optical beams has been predicted and experimentally demonstrated in one-dimensional arrays of the waveguides [11,12]. Another well-known material to manage the beam diffraction is the photonic crystal (PhC), in which the nondiffractive propagation [13] and spatial filtering [14] of optical beams have been considered. Recently, a study of media with gain-loss modulation (GLM) in two dimensions (one longitudinal and one transverse direction) predicted interesting properties of beam propagation [15]. Although the evanescent coupling between adjacent waveguides (formed by the modulation of the refractive index) contributes to the modification of the propagation properties, it is the SD effect supported by the periodic structure that leads to the dependence of the diffraction on the **k** vector of the beam from a physical point of view. Therefore, exploring the physical mechanism of the geometry-induced SD and providing an effective theoretical model for the paraxial beam propagating in artificial materials are crucial and of great significance.

In this work, we theoretically study the propagation of a paraxial beam in two-dimensional (2D) media with SD. A diffraction expression of the paraxial beam is derived. By fitting the dispersion surface of a typical SD medium (a 2D square PhC), the value of the expression is obtained, which determines the beam diffraction. Such a semianalytical method could help us understand and predict the diffraction of the beam that propagates in a SD medium. To confirm our theoretical prediction, we numerically simulate the propagation of a Gaussian beam in the 2-D PhC and compare it with our semianalytical results. It is proved that one can predict the diffraction of a paraxial beam based on the SD theory.

II. THEORETICAL ANALYSIS

The macroscopic Maxwell equations form the basis of the electrodynamics of continuous media [16], and they have to be supplemented by the constitutive equations, which are determined by the response of the medium to the external fields. To quantitatively study the SD, we now consider a time-harmonic field without sources. Under such conditions, the macroscopic Maxwell equations take the form [17]

$$\nabla \times \widehat{\mathbf{E}} = i\omega \widehat{\mathbf{B}}, \tag{1a}$$

$$\nabla \times \widehat{\mathbf{H}} = -i\omega \widehat{\mathbf{D}}, \tag{1b}$$

$$\nabla \cdot \widehat{\mathbf{D}} = 0, \tag{1c}$$

$$\nabla \cdot \widehat{\mathbf{B}} = 0, \tag{1d}$$

*Corresponding author: guoq@scnu.edu.cn

while the constitutive equations in the nonmagnetic dielectric are given by

$$\widehat{\mathbf{D}} = \int \widehat{\varepsilon}(\omega,\mathbf{r}-\mathbf{r}')\widehat{\mathbf{E}}(\omega,\mathbf{r}')d^3\mathbf{r}', \tag{2a}$$

$$\widehat{\mathbf{B}} = \mu_0\widehat{\mathbf{H}}. \tag{2b}$$

For the plane waves, the Maxwell equations become [17,18]

$$\mathbf{k}\times\mathbf{E} = \omega\mathbf{B}, \tag{3a}$$

$$\mathbf{k}\times\mathbf{H} = -\omega\mathbf{D}, \tag{3b}$$

$$\mathbf{k}\cdot\mathbf{D} = 0, \tag{3c}$$

$$\mathbf{k}\cdot\mathbf{B} = 0, \tag{3d}$$

and the corresponding constitutive equations are of the form

$$\mathbf{D} = \varepsilon(\omega,\mathbf{k})\mathbf{E}, \tag{4a}$$

$$\mathbf{B} = \mu_0\mathbf{H}, \tag{4b}$$

which is equivalent to working with spatial Fourier transforms. In Eq. (4a), the permittivity ε depends on the wave vector $\mathbf{k}$, implying that the SD is taken into account.

For 2D media, we have $\partial/\partial y = 0$ (here the $\mathbf{k}$ vector is assumed to be in the x-z plane, i.e., $k_y = 0$); then the Maxwell equations are decomposed into transverse electric (TE) and transverse magnetic (TM) components, i.e.,

$$k_z E_x - k_x E_z = \omega\mu_0 H_y, \tag{5a}$$

$$k_z H_y = \omega\varepsilon(\omega,\mathbf{k})E_x, \tag{5b}$$

$$k_x H_y = -\omega\varepsilon(\omega,\mathbf{k})E_z \tag{5c}$$

for TE waves and

$$k_z E_y = -\omega\mu_0 H_x, \tag{6a}$$

$$k_x E_y = \omega\mu_0 H_z, \tag{6b}$$

$$k_z H_x - k_x H_z = -\omega\varepsilon(\omega,\mathbf{k})E_y \tag{6c}$$

for TM waves. From Eqs. (5) and (6), one can readily get the following equations:

$$\left[k_x^2 + k_z^2 - \omega^2\mu_0\varepsilon(\omega,\mathbf{k})\right]H_y = 0, \tag{7a}$$

$$\left[k_x^2 + k_z^2 - \omega^2\mu_0\varepsilon(\omega,\mathbf{k})\right]E_y = 0. \tag{7b}$$

The above algebraic equations have nontrivial solutions only if their coefficients vanish, i.e.,

$$k_x^2 + k_z^2 - \omega^2\mu_0\varepsilon(\omega,\mathbf{k}) = 0. \tag{8}$$

In general, the SD effect is relatively weak [2,16]; therefore, we expand the permittivity $\varepsilon(\omega,\mathbf{k})$ in a Taylor series with respect to $\mathbf{k}$ around $\mathbf{k}_0 = (k_{x0},k_{z0})$ and keep the low-order terms (linear and quadratic)

$$\begin{aligned}\varepsilon(\omega,\mathbf{k}) &= \varepsilon_0[\varepsilon_c + \alpha_1(k_x - k_{x0}) + \alpha_2(k_z - k_{z0}) \\ &\quad + \alpha_3(k_x - k_{x0})^2 + \alpha_4(k_x - k_{x0})(k_z - k_{z0}) \\ &\quad + \alpha_5(k_z - k_{z0})^2].\end{aligned} \tag{9}$$

Substitution of Eq. (9) into Eq. (8) yields

$$\begin{aligned}k_x^2 + k_z^2 &- \frac{\omega^2}{c^2}[\varepsilon_c + \alpha_1(k_x - k_{x0}) + \alpha_2(k_z - k_{z0}) \\ &+ \alpha_3(k_x - k_{x0})^2 + \alpha_4(k_x - k_{x0})(k_z - k_{z0}) \\ &+ \alpha_5(k_z - k_{z0})^2] = 0,\end{aligned} \tag{10}$$

where $c(=1/\sqrt{\mu_0\varepsilon_0})$ is the speed of light in a vacuum. Equation (10) is the dispersion equation of TE and TM waves.

Without loss of generality, we consider the TE case and discuss the propagation of a paraxial beam, which is a group of TE waves with the same frequency but slightly different propagation directions. The wave vectors of the constituting waves fill a small angle around the central wave vector $\mathbf{k}_0$. It has been shown that if the central wave vector coincides with the z axis of the coordinate system, the evolution of the amplitude envelope $A(x,z)$ of the beam is described by the paraxial wave equation [12,19]

$$i\left(\frac{\partial A}{\partial z} - \gamma\frac{\partial A}{\partial x}\right) - \frac{\delta}{2}\frac{\partial^2 A}{\partial x^2} = 0, \tag{11}$$

where $\gamma = \partial_{k_x}k_z(k_x)|_{k_x=0}$ and $\delta = \partial^2_{k_x}k_z(k_x)|_{k_x=0}$.

Applying the substitution $x' = x + \gamma z$, the second term of Eq. (11) disappears, which means that γ represents a transverse velocity of the beam. Moreover, the parameter δ determines the beam diffraction, which is well known in propagation optics [20,21]. Given a Gaussian beam, where the amplitude in its focus is proportional to $\exp(-x^2/W^2)$, with the focus situated at the entrance facet, the width W will evolve according to [22]

$$W(z) = W_0\sqrt{1 + \left(\frac{2\delta}{W_0^2}z\right)^2}. \tag{12}$$

In order to determine the expressions of γ and δ, in general, one should first find the function $k_z(k_x)$ from the dispersion equation and then obtain its derivation with respect to k_x, which is difficult to realize. Fortunately, we can alternatively get it in an indirect way by differentiating Eq. (10) with respect to k_x, during which k_z is considered an implicit function of k_x. Thus, the following expressions are obtained:

$$\gamma = \frac{\frac{\omega^2}{c^2}\alpha_1}{2k - \frac{\omega^2}{c^2}\alpha_2}, \tag{13a}$$

$$\delta = \frac{-2 - 2\gamma^2 + \frac{2\omega^2}{c^2}(\alpha_3 + \alpha_4\gamma + \alpha_5\gamma^2)}{2k - \frac{\omega^2}{c^2}\alpha_2}, \tag{13b}$$

where ω is the frequency of the incident beam, α_i is the expansion coefficient of the permittivity, and k is the magnitude of the incident central wave vector. Without taking the SD into account, the permittivity is not dependent on the wave vector, so we have $\alpha_i = 0$; then $\gamma = 0$ and $\delta = -1/k$ according to Eq. (13). As a result, Eq. (11) is reduced to the paraxial wave equation in isotropic media. However, when the operating wavelength is not sufficiently large compared to the characteristic length of the media, this assumption fails to work, and the SD should be taken into account, as mentioned previously. Intuitively, the propagation of a paraxial beam in such media will be different.

It is well known that PhCs exhibit strong SD as their characteristic length (the lattice constant) is comparable to the operating wavelength. To show our motivation, we now calculate the values of γ and δ for the beam propagating in a 2D square PhC. The basic structure of the PhC is constructed by arranging square air holes in a silicon slab ($n = 3.5$) with the period $a = 1$ μm and the hole radius $r = 0.3a$. Using the plane-wave method (PWM) [23], we obtain the dispersion

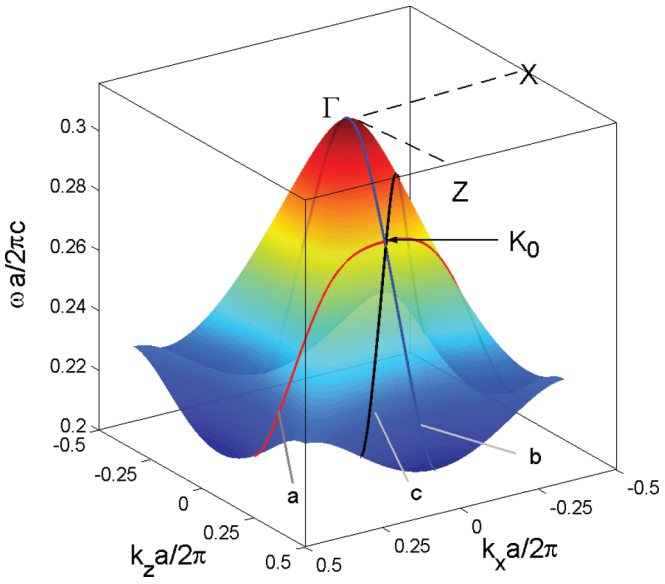

FIG. 1. (Color online) The dispersion surface for the second band of the square PhC.

surface of the PhC and plot its second band in Fig. 1 (TE wave; band 1 is not shown here). To utilize the data of the dispersion surface calculated numerically, we make the following transformation:

$$K = \frac{a}{2\pi}k, \tag{14a}$$

$$\Omega = \frac{\omega a}{2\pi c}, \tag{14b}$$

$$\beta_i = \left(\frac{2\pi}{a}\right)\alpha_i \quad (i = 1,2), \tag{14c}$$

$$\beta_i = \left(\frac{2\pi}{a}\right)^2\alpha_i \quad (i = 3,4,5). \tag{14d}$$

As a result, the dispersion equation (10) turns into

$$\begin{aligned} K_x^2 &+ K_z^2 - \Omega^2[\varepsilon_c + \beta_1(K_x - K_{x0}) + \beta_2(K_z - K_{z0}) \\ &+ \beta_3(K_x - K_{x0})^2 + \beta_4(K_x - K_{x0})(K_z - K_{z0}) \\ &+ \beta_5(K_z - K_{z0})^2] = 0, \end{aligned} \tag{15}$$

and Eq. (13) is transformed to

$$\gamma = \frac{\Omega^2\beta_1}{2K - \Omega^2\beta_2}, \tag{16a}$$

$$\delta = \frac{a}{2\pi}\frac{-2 - 2\gamma^2 + 2\Omega^2(\beta_3 + \beta_4\gamma + \beta_5\gamma^2)}{2K - \Omega^2\beta_2}. \tag{16b}$$

We discuss the beam propagation in two cases with the same width-wavelength ratio R_{WW} but different working frequencies. In the first case, the incident beam with $R_{\mathrm{WW}} = 5$ and $\omega = 0.28 \times 2\pi c/a$ (in band 2) is propagating in the PhC along the Γ-Z direction (see Fig. 1) for 140.2 μm. We have $\mathbf{K}_0 = (K_{x0}, K_{z0}) = (0, 0.212)$, $\Omega = 0.28$, and $K = 0.212$ according to the dispersion surface for this case. By fitting the dispersion surface to Eq. (15) around $\mathbf{K}_0$, the coefficients β_i are obtained as follows: $\beta_1 = 0, \beta_2 = 6.60$, $\beta_3 = 12.93$, $\beta_4 = 0$, and $\beta_5 = 25.24$. To show the fitting effect, we cut the dispersion surface along the transverse, longitudinal, and diagonal directions at the point $\mathbf{K}_0$ and depict the corresponding curves in Fig. 2, where the fitting curves are plotted as dashed red lines. Substituting the above values for the variables in Eq. (16) yields

$$\gamma = 0, \tag{17a}$$

$$\delta = \frac{a}{2\pi}(-0.293) = -0.047\,\mu\mathrm{m}. \tag{17b}$$

By making use of Eqs. (12) and (17b), we obtain the width of the output beam as follows:

$$W(z) = W_0\sqrt{1 + \left(\frac{2\delta}{W_0^2}z\right)^2} = 9.05\,\mu\mathrm{m}, \tag{18}$$

where the incident beam width $W_0 = 8.93$ μm and the propagation distance $z = 140.2$ μm.

In the second case, the incident beam with $R_{\mathrm{WW}} = 5$ and $\omega = 0.14 \times 2\pi c/a$ (in band 1) is propagating in the PhC along Γ-Z for 140.2 μm. Similarly, we have $\mathbf{K}_0 = (K_{x0}, K_{z0}) = (0, 0.410)$, $\Omega = 0.14$, and $K = 0.410$ according to the dispersion surface. By fitting the dispersion surface to Eq. (15) around $\mathbf{K}_0$, the coefficients β_i are obtained, which read as follows: $\beta_1 = 0$, $\beta_2 = 20.96$, $\beta_3 = -25.71$, $\beta_4 = 0$, and $\beta_5 = 55.32$. Substituting the above values for the variables

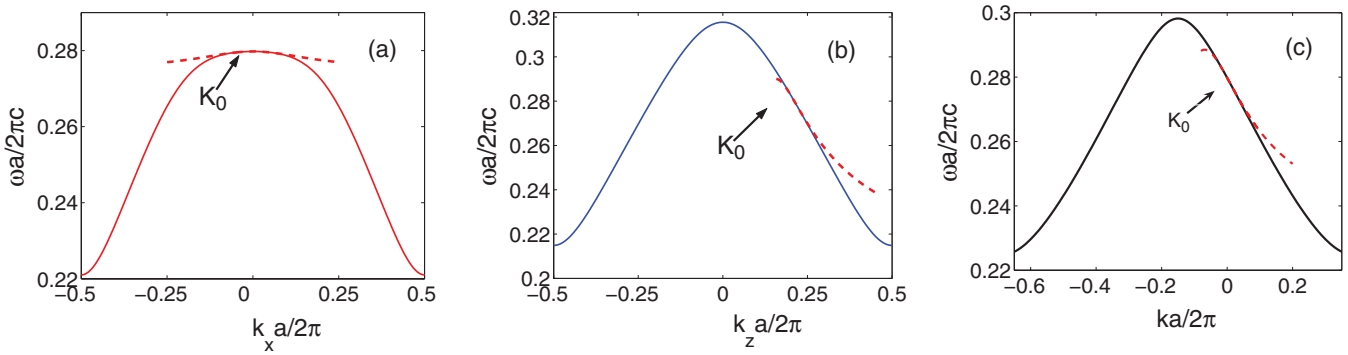

FIG. 2. (Color online) Comparison of the dispersion curves of the square PhC (solid lines) and the fitting curves (dashed red lines) near K_0. (a)–(c) correspond to lines a, b, and c in Fig. 1, respectively.

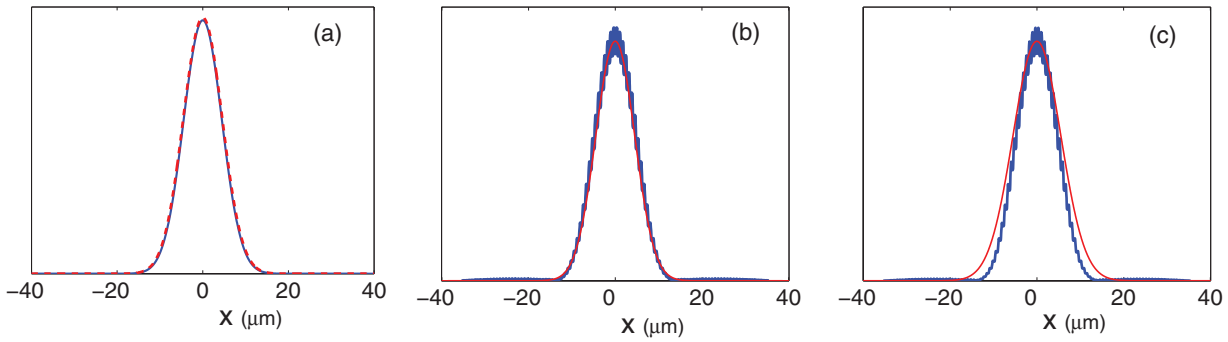

FIG. 3. (Color online) Intensity profile of the beam with $R_{WW} = 5$ and $\omega = 0.28 \times 2\pi c/a$. (a) Comparison of the input intensity profile (solid blue line) and the output intensity profile (dashed red line) based on the theoretical result. (b) Comparison of the numerical simulation [blue (dark gray) line] and the theoretical result [red (light gray) line] of the output intensity profile. (c) Comparison of the output intensity profiles with [blue (dark gray) line, numerical simulation] and without [red (light gray) line] SD.

in Eq. (16) yields

$$\gamma = 0, \tag{19a}$$

$$\delta = \frac{a}{2\pi}(-7.351) = -1.17\,\mu\text{m}. \tag{19b}$$

As a result, the width of the output beam

$$W(z) = W_0\sqrt{1 + \left(\frac{2\delta}{W_0^2}z\right)^2} = 25.62\,\mu\text{m}, \tag{20}$$

where the incident beam width $W_0 = 17.86\ \mu$m and the propagation distance $z = 140.2\ \mu$m.

III. NUMERICAL SIMULATION

To confirm our theoretical results, we now demonstrate the propagation of a Gaussian beam in the 2D square PhC using the finite-difference time-domain (FDTD) method [24], which is an intuitive and accurate tool to test the theoretical results in PhCs. The calculation area is $200 \times 400a$ with a grid size of $1/25a$. A Gaussian beam with magnetic field parallel to the holes (TE waves) is launched into the PhC at the focus along Γ-Z.

We simulate the beam propagation in two situations corresponding to the cases discussed in Sec. II. The results are presented in Figs. 3 and 4 . As shown in Fig. 3(a), the case of $R_{WW} = 5$ and $\omega = 0.28 \times 2\pi c/a$ does not show significant variation after propagating 140.2 μm, while Fig. 4(a) indicates that the beam with the same R_{WW} and propagation distance except for $\omega = 0.14 \times 2\pi c/a$ expands. To show the consistence between the theoretical prediction and the numerical simulations, we plot the intensity profiles of the output beam based on the theoretical results and the numerical simulations in Figs. 3(b) and 4(b) for comparison, where we normalized their maximums to the same value. To show the SD effect, we add Figs. 3(c) and 4(c) to compare the output intensity profiles with and without SD [25]. The results show that the SD produces an opposite effect to the beam that propagates in media without SD. The reason is that the SD effect is strongly dependent on the dimensionless parameter a/λ, as previously mentioned. A change of the frequency (or, equivalently, the wavelength) leads to a change of SD, which alters the beam propagation property. Unlike the isotropic uniform media, the SD media can reduce, increase, and even cancel the beam diffraction (well known). To quantitatively compare the theoretical prediction and the numerical simulations, we calculate the statistical widths (defined as the second-order moment widths [26]) of the output beam in the numerical simulations. After a simple calculation, it is found that the statistical widths of the output beam are 9.16 and 26.25 μm, respectively, which are close to the theoretical results.

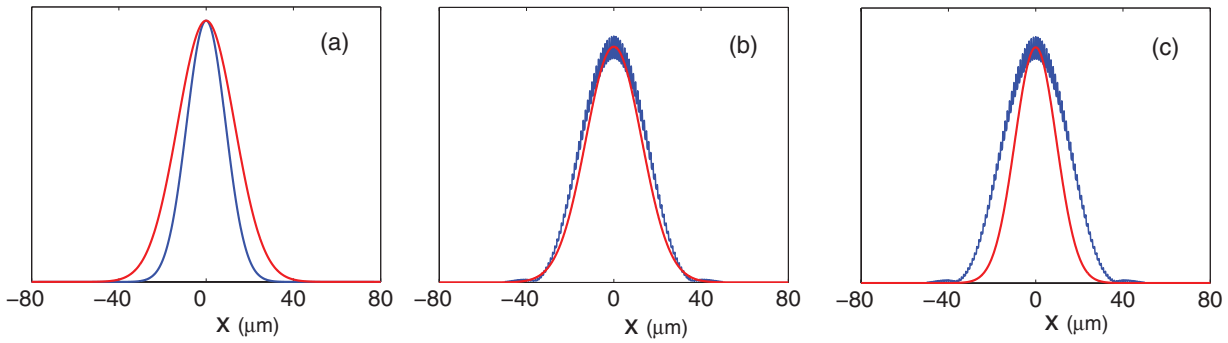

FIG. 4. (Color online) Intensity profile of the beam with $R_{WW} = 5$ and $\omega = 0.14 \times 2\pi c/a$. (a) Comparison of the input intensity profile [blue (dark gray) line] and the output intensity profile [red (light gray) line] based on the theoretical result. (b) Comparison of the numerical simulation [blue (dark gray) line] and the theoretical result [red (light gray) line] of the output intensity profile. (c) Comparison of the output intensity profiles with [blue (dark gray) line, numerical simulation] and without [red (light gray) line] SD.

IV. CONCLUSION

In conclusion, the theory of a paraxial beam propagating in 2D media with SD is discussed. We address the idea that the SD, which leads to the dependence of the propagation properties of a beam on its **k** vector, originates from the dependence of the permittivity on the wave vector. By expanding the permittivity $\varepsilon(\omega,\mathbf{k})$ with respect to **k**, we get a dispersion equation of waves containing the expansion coefficients. Furthermore, based on the dispersion equation and the paraxial condition, we obtain a diffraction expression of the paraxial beam. By fitting the dispersion surface of a typical SD medium (a 2D PhC, for example), the value of the expression is determined, with which one can predict the diffraction of a paraxial beam. Numerical simulations confirm the theoretical prediction. The presented analysis, which considers 2D media with SD, could be also extended to the three-dimensional (3D) case. For the 3D case, the dispersion equation obtained by Taylor expansion includes three components of the wave vector, which is fit to the dispersion surface of a 3D medium with SD. At the same time, the longitudinal wave vector k_z is a function of two transverse wave vectors, k_x and k_y, so one needs to differentiate the dispersion equation with respect to k_x and k_y to obtain the diffraction expression [19]. We expect that our results would pave the way for advanced manipulation of optical beams in artificial SD media.

It is worth stressing that the discussions put forward here are different from previous studies on this topic [13–15], which considered several specific beam propagation phenomena (not quantitative), such as self-collimation (diffraction-free propagation) [13,15] and spatial filtering (superdiffusion) [14,15], in PhCs and in media with GLM. In contrast, our results are more general, and the semianalytical method can be applied to normal, canceled, and anomalous diffraction. Especially, one can quantitatively determine the beam diffraction and get the output beam profile based on our theoretical prediction. Furthermore, the semianalytical approach here is independent of the type of modulation. The effect of modulation is included in the diffraction expression, whose value can be obtained by fitting the exact dispersion surface.

ACKNOWLEDGMENTS

This research was supported by the National Natural Science Foundation of China (Grants No. 11074080 and No. 11274125), the Natural Science Foundation of Guangdong Province of China (Grant No. S2012010009178), the Hunan Provincial Natural Science Foundation of China (Grant No. 13JJ4097), and the Construct Program of the Key Discipline in Hunan Province of China.

[1] V. L. Ginzburg, Zh. Eksp. Teor. Fiz. **34**, 1593 (1958) [Sov. Phys. JETP **7**, 1096 (1958)].
[2] V. M. Agranovich and V. L. Ginzburg, *Crystal Optics with Spatial Dispersion, and Excitons*, 2nd ed. (Springer, Berlin, 1984).
[3] A. I. Căbuz, D. Felbacq, and D. Cassagne, Phys. Rev. A **77**, 013807 (2008).
[4] D. W. Prather, S. Shi, J. Murakowski, G. J. Schneider, A. Sharkawy, C. Chen, B. Miao, and R. Martin, J. Phys. D **40**, 2635 (2007).
[5] P. A. Belov, R. Marques, S. I. Maslovski, I. S. Nefedov, M. Silveirinha, C. R. Simovski, and S. A. Tretyakov, Phys. Rev. B **67**, 113103 (2003).
[6] G. Bouchitte and D. Felbacq, SIAM J. Appl. Math. **66**, 2061 (2006).
[7] M. A. Shapiro, G. Shvets, J. R. Sirigiri, and R. J. Temkin, Opt. Lett. **31**, 2051 (2006).
[8] S. Noda, M. Yokoyama, M. Imada, A. Chutinan, and M. Mochizuki, Science **293**, 1123 (2001).
[9] Y. Xu, X. Chen, S. Lan, Q. Dai, Q. Guo, and L. Wu, Opt. Express **17**, 4903 (2009).
[10] D. Tang, L. Chen, and W. Ding, Appl. Phys. Lett. **89**, 131120 (2006).
[11] H. S. Eisenberg, Y. Silberberg, R. Morandotti, and J. S. Aitchison, Phys. Rev. Lett. **85**, 1863 (2000).
[12] T. Pertsch, T. Zentgraf, U. Peschel, A. Bräuer, and F. Lederer, Phys. Rev. Lett. **88**, 093901 (2002).
[13] K. Staliunas and R. Herrero, Phys. Rev. E **73**, 016601 (2006).
[14] K. Staliunas and V. J. Sánchez-Morcillo, Phys. Rev. A **79**, 053807 (2009).
[15] K. Staliunas, R. Herrero, and R. Vilaseca, Phys. Rev. A **80**, 013821 (2009).
[16] L. D. Landau, E. M. Lifshitz, and L. P. Pitaevskii, *Electrodynamics of Continuous Media*, 2nd ed. (Pergamon, Oxford, 1984).
[17] J. A. Kong, *Electromagnetic Wave Theory* (EMW Publishing, Cambridge, MA, 2000).
[18] V. M. Agranovich and Y. N. Gartstein, Phys. Usp. **49**, 1029 (2006).
[19] Q. Guo and S. Chi, J. Opt. A **2**, 5 (2000).
[20] H. A. Haus, *Waves and Fields in Optoelectronics* (Prentice-Hall, Englewood Cliffs, NJ, 1984).
[21] G. P. Agrawal, *Nonlinear Fiber Optics* (Academic, New York, 1995).
[22] M. Born and E. Wolf, *Principles of Optics*, 6th ed. (Pergamon, Oxford, 1987).
[23] S. G. Johnson and J. D. Joannopoulos, Opt. Express **8**, 173 (2001).
[24] A. Taflove and S. C. Hagness, *Computational Electrodynamics* (Artech House, Norwood, MA, 2000).
[25] The refractive index here is considered the effective refractive index.
[26] A. E. Siegman, *Lasers* (University Science Books, Mill Valley, CA, 1986).